WIRELESS TRANSMITTER FOR OPTICAL COMMUNICATION WITH FREQUENCY-MODULATED LASER CARRIER

Marian PEARSICĂ, Laurian GHERMAN

"Henri Coanda" Air Force Academy, Braşov, Romania (marianpearsica@yahoo.com, lauriang@gmail.com)

DOI: 10.19062/1842-9238.2023.21.2.7

Abstract: *Interest in the use of unguided optical systems is growing, due to the development of wireless mobile and indoor communication systems as well as the applications of lasers in space technology. The proposed laser transmitter, with frequency-modulated carrier, represents the optical transmitter of a wireless optical communication system, for transmitting audio signals on laser carriers, which can be used both inside buildings and outside, for distances estimated according to system parameters. In the paper are presented elements of design of the electrical diagram of principle, as well as analysis by SPICE simulation of the designed circuit. The results obtained by SPICE simulation synthesize the operation of the laser transmitter, allowing an optimization of the parameters of the component circuits.*

Keywords: *wireless transmitter, laser carrier, MF modulator, optical transmitter*

1. INTRODUCTION

Optical communication systems offer a broad spectrum of possibilities due to the diverse modulation and detection methods [3,6], types of optical channels, and operating conditions. This encompasses interior optical communication systems, primarily utilizing laser diodes and light-emitting diodes as optical sources for transmission [5,8,10]. The modulation process involves the excitation mechanism, wherein the optical signal is modulated with a pulse-modulated subcarrier.

Unguided optical communications find applications both indoors and in external short links [1,2,4]. Designing outdoor optical communication systems requires consideration of the significant atmospheric attenuation variations due to changing weather conditions. The input information undergoes encoding and is applied to a modulator excitation device, steering the electro-optical modulator. This modulator, positioned inside or outside the laser cavity, modulates the laser beam.

The modulated laser beam is collimated by the transmitting optical antenna, traverses the transmission medium (such as vacuum space, atmosphere, controlled atmosphere guide, or optical fiber), and is captured by the receiving optical antenna [1,7,9]. The concentrated laser radiation is then directed to an optical receiver. At the photodetector's output, an electrical signal is obtained through direct detection or heterodyne detection, which undergoes further processing in a radio receiver. The resulting signal is decoded, yielding the output information.

The modulation of the optical carrier distinguishes itself from radio frequency carrier modulation due to different processes, characteristics, and parameters of the optoelectronic devices involved.

Frequency modulation offers a notable advantage as its inherent detection scheme eliminates noise, provided the received signal surpasses noise sources.

Transmitting information through frequency variations, rather than amplitude changes, ensures a noise-resistant signal at the audio receiver, particularly in the presence of electromagnetic interference and scintillations.

2. PRINCIPLE OF OPERATION

The core of the laser transmitter is a voltage-controlled oscillator, comprising an integration circuit and a hysteresis comparator [3]. This element executes frequency modulation of audio signals (20*Hz*-16*kHz*), generating a pulsed signal output with a frequency ranging from 140*kHz* to 260*kHz*, with the carrier signal frequency set at 200*kHz*.

The FM modulator [3,6], a voltage-controlled oscillator, switches the laser diode between two discrete current levels, incorporating encoded information into the laser diode driver's signal. This process generates a frequency-modulated subcarrier wave, essentially a position pulse modulation (PPM) signal operating at around 100*kHz*. The supply current to the laser diode is adjustable within the range of 0-20*mA*.

A voltage regulator provides the supply current to the laser diode via the laser driver, resulting in the emission of coherent, wavelength laser beams with specific characteristics. The laser diode emits optical pulses synchronized with the PPM subcarrier. The audio amplifier circuit amplifies and isolates the input signal, transmitting it to the modulation circuit.

The voltage-controlled oscillator, operating at a frequency of 200*kHz*, comprises an integrator (CI_3) and a hysteresis comparator circuit (CI_4), serving a critical role in the modulation process (Fig. 1).

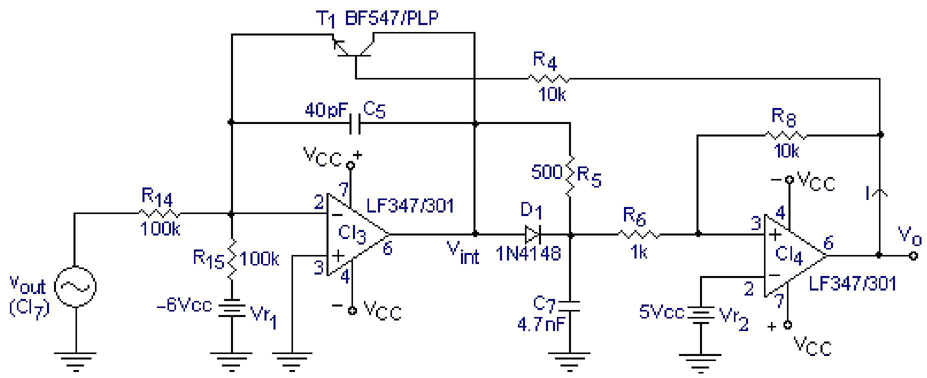

FIG. 1. Wiring diagram of the voltage-controlled oscillator

The reference voltage (V_{r2}) of the hysteresis comparator has been set at 5*Vcc*. The comparator output voltage is, $V_o \in \{V_{oH}; V_{oL}\}$ where, $V_{oH} = 12V$ and $V_{oL} = -12V$. The comparator switches when $V_+ = V_{r2}$. Current *I* (FIG. 1) is determined with the relations:

$$I = \frac{V_{oH} - V_{in}}{R_6 + R_8} = \frac{V_{oH} - V_{r2}}{R_8} \quad \Rightarrow \quad V_{in} = \frac{V_{r2}(R_6 + R_8) - V_{oH} R_6}{R_8} = V_{r2}\left(1 + \frac{R_6}{R_8}\right) - V_{oH}\frac{R_6}{R_8} \tag{1}$$

For integration levels, the following values are obtained:

$$V_{PL} = V_{r2}\left(1 + \frac{R_6}{R_8}\right) - V_{oH}\frac{R_6}{R_8} \cong 4{,}3V \tag{2}$$

$$V_{PH} = V_{r2}\left(1+\frac{R_6}{R_8}\right) - V_{oL}\frac{R_6}{R_8} \cong 6{,}7V \tag{3}$$

The upper integration limit is given by the V_{PH} voltage plus the voltage falling on diode D_1, resulting in approximately 6,7*V*, as seen from the waveforms obtained by simulation. The high-frequency transistor T_1, connected in bypass to the integration capacitor C_5, provides the discharge path of the capacitor, which discharges completely in a very short time, fixed to $0{,}5\mu s$.

The voltage at the output of the integrator, for $V_{out} = 0$ (V_{out} is the voltage at the output of the audio amplification circuit), is given by:

$$V_{\text{int}} = -\frac{1}{R_{15}C_5}\int V_{r1}dt = \frac{6}{100\cdot 10^3 \cdot C_5}\cdot t = 6{,}7V \tag{4}$$

For a subcarrier frequency of 200*kHz* and taking into account the discharge time of the integration capacitor, the integration time results, $t = 4{,}5\mu s$.

Through the audio signal amplification circuit (achieves frequency-dependent amplification at 20*dB/dec*), the audio signal frequency is practically converted into a voltage level ($V_{out} \neq 0$), which is applied to the integrator input, summing up with the DC voltage $V_{r1} = -6V$. Thus, depending on the V_{out} value, the integration slope changes, resulting in frequency modulation of the 200*kHz* subcarrier.

The voltage at the output of the integrator, for, $V_{out} \neq 0$ is given by:

$$V_{\text{int}} = -\frac{1}{R_{15}C_5}\int V_{r1}dt - \frac{1}{R_{14}C_5}\int V_{out}dt = -\frac{1}{RC_5}\int\left(V_r + V_{out}\right)dt = 6{,}7V \tag{5}$$

The maximum amplitude of the V_{out} signal (obtained at the frequency of 16*kHz)* has been set at 2*V* (above this value the distortion of the signal that controls the power supply of the laser diode is observed). Substituting in relation (5) and taking into account the phase of the audio signal, results in the maximum time, respectively, the minimum integration time: $t_{\min} = 3{,}3\mu s$; $t_{\max} = 6{,}6\mu s$.

The limit frequencies of the FM-modulated subcarrier shall be determined:

$$T_{\min} = t_{\min} + t_{desc} = 3{,}8\mu s \quad \Rightarrow \quad f_{\max} = \frac{1}{T_{\min}} \cong 260kHz \tag{6}$$

$$T_{\max} = t_{\max} + t_{desc} = 7{,}1\mu s \quad \Rightarrow \quad f_{\min} = \frac{1}{T_{\max}} \cong 140kHz \tag{7}$$

The division circuit (bistable type D) (CI_{6A} – FIG. 2) divides the frequency of the V_o signal by 2 and restores symmetry. It follows that the signal frequency at the output of the frequency divider is between 70k*Hz* and 130*kHz.*

3. SPICE ANALYSIS OF DESIGNED SUBSYSTEMS

The SPICE analysis diagram of the laser transmitter for audio signals, with frequency-modulated subcarrier, is shown in Fig. 2.

The frequency simulation was performed taking into account the transfer functions of the analyzed circuits. Time domain analysis was performed over several periods of time, obtaining waveforms for electrical signals in the circuit.

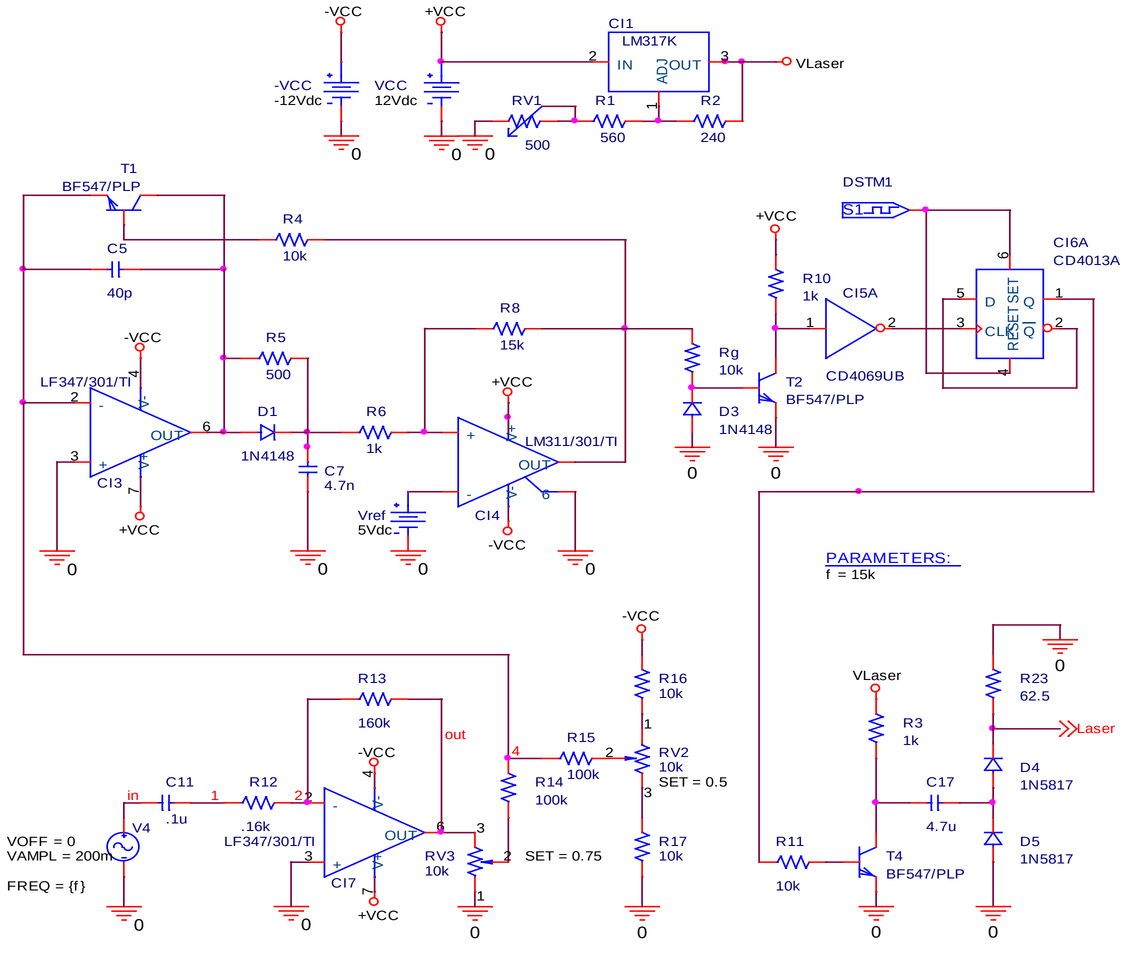

FIG. 2. SPICE Analysis Diagram of the Laser Transmitter

Figure 3 shows the frequency response of the audio signal amplification circuit. It is noticed that the amplification of audio signals is 20*dB/dec*, the maximum amplification of 60*dB*, obtaining at a frequency of about 20*kHz*.

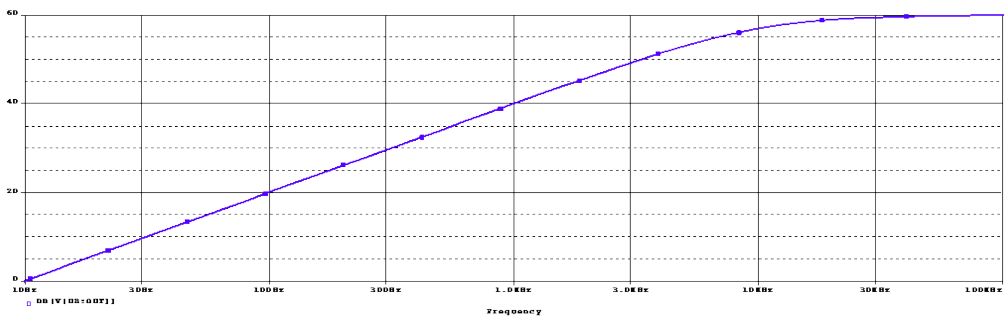

FIG. 3. Frequency analysis of audio signal amplification circuit

Below are presented the waveforms for the analyzed circuit, namely: the signal from the output of the amplifier circuit (V_{out} – violet), the signal from the integrator output (V_{int} – blue), the signal from the comparator output (V_o – red) and the supply voltage of the laser diode (green).

Figure 4 shows the waveforms for $V_{out} = 0$. It is noticed that in this case the oscillation frequency of the oscillator controlled in voltage is 200*kHz*, and the frequency of the laser supply current is 100*kHz*. The maximum voltage at the integrator output is 6,1*V* and the laser supply voltage is 2,5*V*, resulting in a maximum supply current of 40*mA*.

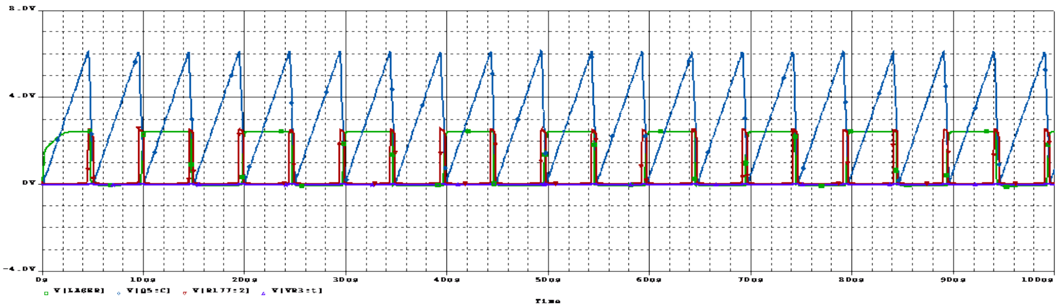

FIG. 4. Waveforms for $V_{out} = 0$

Figures 5 and 6 show waveforms for $V_{out} \neq 0$ $(V_{AMPL} = 200mV)$, at modulating audio signal frequencies of 5*kHz* and 16*kHz*, respectively.

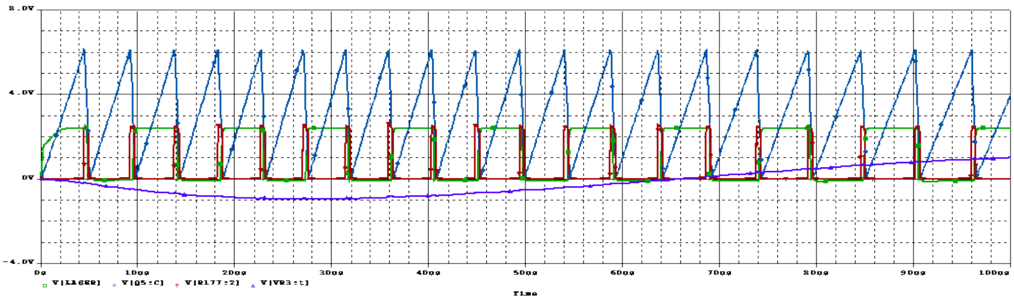

FIG. 5. Waveforms for $V_{out} \neq 0$, $f = 5kHz$

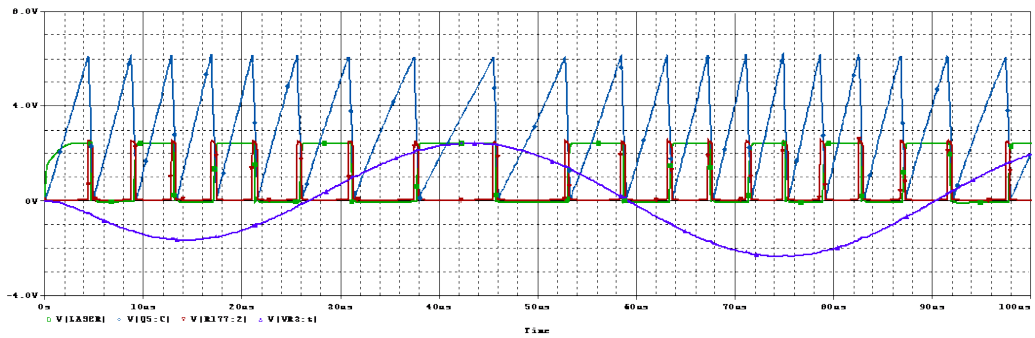

FIG. 6. Waveforms for $V_{out} \neq 0$, $f = 16kHz$

From the analysis of the waveforms presented it can be seen that the frequency of the MF subcarrier depends on the frequency of the audio signal, which varies between 70*kHz* and 130*kHz*.

Figure 7 shows the waveforms for a $V_{AMPL} = 250mV$ (f = 16kHz) input signal applied to the input of the amplifier circuit. The amplitude of the signal applied to the input of the integrator circuit (CI_3), through the resistive divider made with RV_3, represents 1/4 of the signal at the output of the line amplifier (CI_7). It is noticed that the line amplifier saturates, which has the effect of distorting the received signal. The higher the voltage at the output of the line amplifier, the more distorted the received signal will be.

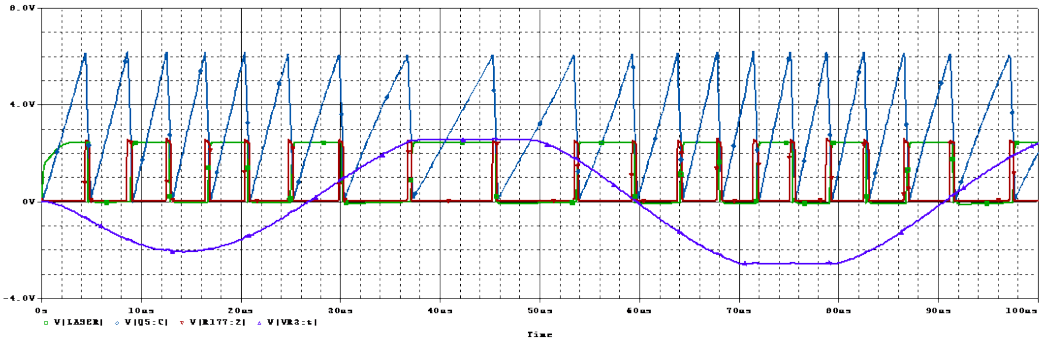

FIG. 7. Waveforms for $V_{AMPL} = 250mV$, f = 16kHz

Figure 8 shows waveforms for a 500mV audio signal with a frequency of 16kHz. Stronger saturation of the line amplifier is observed.

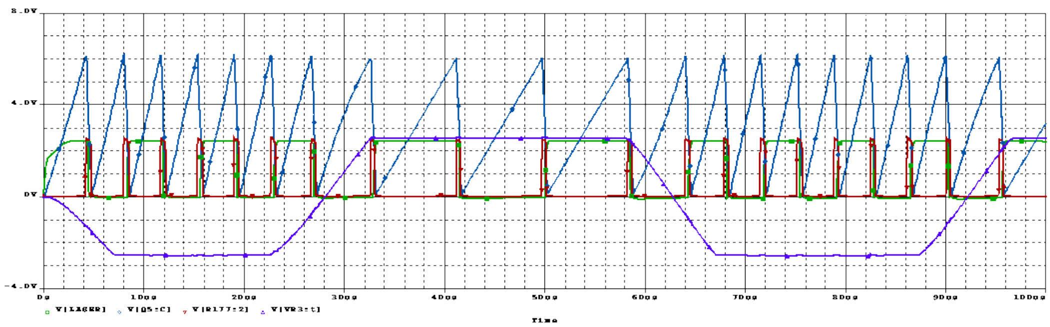

FIG. 8. Waveforms for $V_{AMPL} = 500mV$, f = 16kHz

CONCLUSIONS

The configuration of a laser transmitter is fundamentally dictated by the chosen optical modulation method, the transmission medium, and the targeted range. In this context, frequency modulation has been selected as the modulation method, with the Medium Frequency (MF) frequency-modulated signal adopting Pulse Position Modulation (PPM). The PPM signal is characterized by pulsed signals, where the pulse position is proportionate to the amplitude of the analog modulating signal. Specifically, the MF signal is derived from the Pulse Width Modulation (PWM) signal, generating pulses with a fixed duration corresponding to the rising edge of the PWM signal pulses. This mechanism results in pulses whose positioning is contingent upon the analog input signal.

Following an in-depth SPICE analysis, conducted for a subcarrier frequency of 200kHz and established reference voltage levels V_{r1} (–6Vcc) and V_{ref} at the comparator CI_4 (5Vcc), it was determined that the maximum amplitude of the signal at the output of the audio amplification circuit should be carefully controlled to avoid distortion of the MF signal.

The frequency-modulated carrier operates above the audio frequency band, strategically positioned outside the frequency bands associated with ambient noise perception. This placement minimizes the impact of potential sources of disturbances, as these disturbances exhibit low levels in the pass band of a meticulously designed receiver operating at ultrasonic frequencies. Additionally, the frequency-modulated subcarrier displays robust immunity to detecting nonlinearity in photodetectors.

The waveforms obtained through SPICE simulations, both in the time domain and frequency domain (amplitudes, periods, amplifications, etc.), correspond remarkably well with the theoretical results derived during the design phase. This alignment serves as a robust verification of the functionality and stability of the proposed system. Moreover, the designed system underwent experimental validation, demonstrating a commendable concordance between the experimental and theoretical results obtained during the design phase, as well as alignment between the experimentally acquired waveforms and those obtained through SPICE simulation. This comprehensive validation process underscores the reliability and efficacy of the designed laser transmitter system.

REFERENCES

[1] H. Henniger and O. Wilfert, An Introduction to Free-Space Optical Communications, *Radioengineering*, vol. 19, no. 2, pp. 203-2012, June 2010;

[2] S. Hranilovic, *Wireless Optical Communication Systems*, McMaster University, Hamilton, Springer Science Ontario, Canada, 2006;

[3] M. Carter, Laser Pointer Audio Modulator - Laser Beam Detector/Demodulator, Available: http://www.maxcarter.com; www.maxmcarter.com/lasrstuf/lasermodulator.html;

[4] A.K. Majumdar and J.C. Ricklin, *Free-Space Laser Communications. Principles and Theory*, New York (USA), Springer, 2008;

[5] L.U. Khan, *Visible light communication: Applications, architecture, standardization and research challenges*, *Digital Communication Networks*, vol. 3(2) pp. 78-88, 2016;

[6] G. Yan, W. Min and D. Weifeng, Performance Research of Modulation for Optical Wireless Communication System, *Journal of Networks*, vol. 6, no. 8, August 2011;

[7] N. N. Puşcaş, *Sisteme de comunicaţii optice*, Editura Matrix Rom, Bucureşti, 2006;

[8] S. Dimitrov and H. Haas, *Principles of LED Light Communications: Towards Networked Light Fidelity*, Cambridge University Press, March 2015;

[9] Z. Ghassemlooy, P. Luo and S. Zvanovec, *Optical Camera Communications*, Springer, pp 547-568, 2016;

[10] P.H. Pathak, X. Feng, P. Hu and P. Mohapatra, Visible light communication, networking, and sensing: a survey, potential and challenges, *IEEE Communications Surveys & Tutorials*, vol. 17, no. 4, pp. 2047-2077, 2015.